Configurational Continuum modelling of crystalline surface evolution

Navot Israeli and Daniel Kandel

Abstract. We propose a novel approach to continuum modelling of dynamics of crystal surfaces. Our model follows the evolution of an ensemble of step configurations, which are consistent with the macroscopic surface profile. Contrary to the usual approach where the continuum limit is achieved when typical surface features consist of many steps, our continuum limit is approached when the number of step configurations of the ensemble is very large. The model is capable of handling singular surface structures such as corners and facets and has a clear computational advantage over discrete models.

Keywords. continuum modelling, multi scale modelling, step flow, surface evolution.

1. Introduction

The behavior of classical physical systems is typically described in terms of equations of motion for discrete microscopic objects (e.g. atoms). The dynamics of the microscopic objects is usually very erratic and complex. Nevertheless, in many cases a smooth behavior emerges when the system is observed on macroscopic length and time scales (e.g. in fluid flow through a pipe). A fundamental problem in physics is to understand the emergence of the smooth macroscopic behavior of a system starting from its microscopic description. A useful way to address this problem is to construct a continuum, coarse-grained model, which treats the dynamics of the macroscopic, smoothly varying, degrees of freedom rather than the microscopic ones. The derivation of continuum models from the microscopic dynamics is far from trivial. In most cases it is done in a phenomenological manner by introducing various uncontrolled approximations.

In this work we address the above problem in the context of the dynamics of crystal surfaces. The evolution of crystal surfaces below the roughening transition

proceeds by the motion of discrete atomic steps which are separated by high symmetry orientation terraces. One can model step motion by solving the diffusion problem of adatoms on the terraces with appropriate boundary conditions at step edges. This approach was introduced long ago by Burton, Cabrera and Frank [1], and was further developed by other authors [2]. The resulting models specify the normal velocity of each step in the system as a function of its position and shape and as a function of position and shapes of neighboring steps. These step flow models are capable of describing surface evolution on the mesoscopic scale with significant success [3, 4]. However, step flow models pose a serious challenge for numerical computations, and can be solved only for small systems.

Several attempts were made to construct continuum models for stepped surfaces [5, 6, 7, 8, 9, 10, 11, 12, 13, 14, 15, 16, 17, 18], in order to understand their large scale properties. The general idea behind these attempts is that step flow can be treated continuously in regions where every morphological surface feature is composed of many steps. If we label surface steps by the index n, the continuum limit in these models is obtained by taking n to be continuous. In what follows we will refer to these models as the *conventional* approach.

In the literature, there are two methods to derive conventional continuum models. One method is to write down the discrete step equations of motion and then transform them into a partial differential equation by taking the step index n to be continuous [7, 12, 13, 14, 15]. The second method is to start with a continuous surface free energy density and derive a surface dynamic equation that minimizes it[6, 8, 11, 16, 17, 18]. These two methods are complementary provided that: 1. The free energy density of the second method is the continuum analog of the free energy of an array of discrete steps. 2. The two methods uses the same mass transport mechanism. Such continuum models are fairly successful in describing the evolution of smooth surfaces with very simple morphologies. However, they suffer from fundamental drawbacks, which do not allow generalizations to more complex and realistic situations.

The most severe drawback is that below the roughening temperature, crystal surfaces have singularities in the form of corners and macroscopic facets. The latter are a manifestation of the cusp singularity of the surface free energy at high symmetry crystal orientations. The assumption that every surface feature is composed of many steps clearly breaks down on macroscopic facets where there are no steps at all. Thus, existing continuum models fail conceptually near singular regions. Several authors have tried to overcome this problem by solving a continuum model only in the non-singular parts of the surface and then carefully match the boundary conditions at the singular points or lines[11, 14, 13, 15]. In most cases however it is not at all clear how these matching conditions can be derived. This difficulty is a fundamental drawback of conventional continuum models and not merely a technicality. As we argue below, boundary conditions at the singular points or lines cannot be derived in the context of conventional continuum models.

To see why this is true consider the situation near a facet edge. The step at the facet edge is special and obeys a unique equation of motion. In contrast to steps

in the sloping parts of the surface which all have two neighboring steps of the same sign, a facet step has only one neighbor of the same sign and potentially a second neighbor of an opposite sign. There might also be special physical conditions such as surface reconstruction that add to the uniqueness of a facet step. As we found in several cases [12, 13, 14, 15], the unique behavior of a facet step sensitively determines the amount of material emitted or absorbed at the facet and the rate at which steps cross the facet and annihilate. When going to the continuum limit these quantities serve as flux boundary conditions at the singularity. The problem is that conventional continuum models are derived from the equations of motion (or from the surface free energy density) that apply away from the facet and are therefore ignorant of the special behavior of facet steps. Thus, the boundary conditions at the facet edge must be derived from a careful analysis of the discrete dynamics of faces steps. However, in going to the continuum in the conventional way, one loses the information regarding the position of individual steps and the discrete analysis cannot be performed.

Another approach for dealing with surface singularities is to round the surface free energy cusp [16, 17, 18], approximating true facets by relatively flat but analytic regions. This method avoids the need of specifying explicit boundary conditions at the singularity by assuming analyticity of the surface. The correct surface behavior is then expected to be captured in the limit of vanishing cusp rounding. This procedure completely ignores the key role of facet steps and implicitly assumes that the surface free energy derived for non singular orientations determines the dynamics on facets as well. This assumption is generally false due to the same reasons discussed above. An example for a case where cusp rounding leads to erroneous results can be found in Appendix A.

In this work we propose a conceptually new definition of the continuum limit, which we term Configurational Continuum[19]. Configurational Continuum allows construction of continuum models, which are free of all the limitations of conventional continuum models discussed above. It provides a rigorous way of deriving the continuum model directly from the discrete step equations of motion. Like other continuum models, Configurational Continuum has a clear computational advantage over the discrete step model due to the small number of discretization points it requires for the description of smooth surface regions in a numerical scheme.

2. Configurational continuum

In order to overcome the limitations of conventional continuum models we now propose a conceptually new definition of the continuum limit for stepped surfaces. Our key observation is that a continuous surface height profile can be represented by many similar, but not identical, step configurations. Figure 1 is a one dimensional demonstration of this point. It shows a continuous height function, $h(x)$, of position x (thick solid line), and three valid microscopic representations of this

profile as step configurations. The main idea of this work is to define the height profile in the continuum limit as the upper envelope of the discrete height functions of an *ensemble* of many such step configurations.

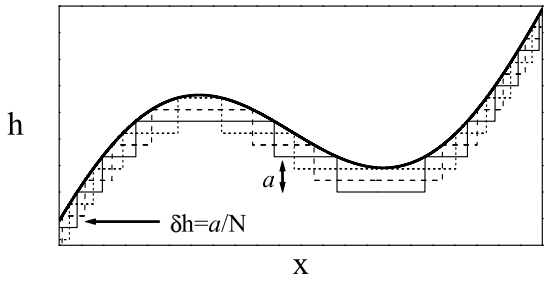

FIGURE 1. A schematic illustration of the ensemble of configurations whose upper envelope defines the continuum limit.

To construct the configurations of the ensemble let a be the height of a single step and N the number of configurations in the ensemble. We construct the ensemble so that the height difference δh, between two adjacent configurations is a/N, as depicted in Fig. 1. The continuum limit is obtained when $N \to \infty$. The generalization to higher dimensions is straightforward.

The dynamics of the continuum model is as follows. Each step configuration of the ensemble evolves according to the microscopic dynamics. As a result, the envelope of discrete height functions changes with time, thus defining the evolution of the continuous height function $h(\vec{r})$ where $\vec{r}$ is a vector in the high symmetry xy plane. There is one technical complication which might arise if two steps from different configurations cross each other. Such an event would make $h(\vec{r})$ a multi valued function of position and requires a more general mathematical description of the surface. For simplicity we ignore this and assume that $h(\vec{r})$ remains single valued.

There is a crucial assumption hidden in this definition of the continuum model. We postulate that our construction leads to a mathematically well defined height function at all times. When does this assumptions hold? Consider two initially similar configurations of the ensemble. Our continuum limit is well defined provided these two configurations have similar microscopic dynamics and hence remain similar at later times. Note however that this assumption has to hold in the conventional continuum definition as well, and therefore does not put additional restrictions on our model. In fact, if two initially similar configurations evolve very differently, one must abandon the continuum limit and follow the specific microscopic configuration of interest, using discrete dynamics.

We now derive the evolution equation for the continuous height, $h(\vec{r},t)$, at position $\vec{r}$ and time t. As a basis for the derivation we assume knowledge of the discrete equations of motion for the underlying step flow model. These equations of motion specify the normal velocity of a step that passes through $(\vec{r},t)$ as a function of the local step configuration. We denote this dependency by writing

$$\vec{v}\left(\vec{r},t\right)=\vec{v}\left(C_{\vec{r},t}\right), \tag{2.1}$$

where $C_{\vec{r},t}$ denotes the configuration of steps in the region that influences the step velocity at $(\vec{r},t)$. In most models of step flow this region of influence covers a small number of neighboring steps. Note that in the context of the discrete step model, $C_{\vec{r},t}$ is the actual configuration of steps in the system. When going to the continuum we will be interested in the ensemble of configurations $\{C_{\vec{r},t}\}$ which are consistent with $h(\vec{r},t)$.

The continuous height $h(\vec{r},t)$ changes with time due to the flow of steps through $\vec{r}$, and due to nucleation and annihilation of steps. At this stage we disregard nucleation processes and include them later. First, we consider positions which are not local extrema of the height profile. It is obvious from the construction of the Configurational Continuum, that for each point $\vec{r}$ there is exactly one configuration $C_{\vec{r},t}$ in the ensemble, which has a step that passes through $\vec{r}$ at time t. That step lies along the unique equal-height contour line, which passes through $\vec{r}$. As is demonstrated in Fig. 1, the exact positions of neighboring steps in the configuration $C_{\vec{r},t}$ can be calculated from the knowledge of $h(\vec{r},t)$, and the fact that in this configuration there is a step at $\vec{r}$. Hence, we can use the discrete step model Eq. (2.1) and calculate the normal velocity of the step $\vec{v}\left(C_{\vec{r},t}\right)$. Note that at different positions, $\vec{v}\left(C_{\vec{r},t}\right)$ is the normal velocity of steps which may belong to *different* configurations in the ensemble.

Next we define the directional gradient in the direction from which steps flow towards $\vec{r}$

$$\nabla h_{-\hat{v}}(\vec{r},t)\equiv-\hat{v}(\vec{r},t)\lim_{\epsilon\to0_{+}}\frac{h\left(\vec{r}-\epsilon\cdot\hat{v}(\vec{r},t)\right)-h\left(\vec{r},t\right)}{\epsilon}, \tag{2.2}$$

where $\hat{v}(\vec{r},t)=\frac{\vec{v}\left(C_{\vec{r},t}\right)}{\left|\vec{v}\left(C_{\vec{r},t}\right)\right|}$. This is useful for the calculation of the current of steps arriving at $\vec{r}$:

$$J(\vec{r},t)=\frac{N}{a}\left|\nabla h_{-\hat{v}}(\vec{r},t)\cdot\vec{v}\left(C_{\vec{r},t}\right)\right|, \tag{2.3}$$

where we have used the fact that the local step density is $\left|\nabla h_{-\hat{v}}(\vec{r},t)\right|N/a$. Note that J is the current of steps belonging to all configurations in the ensemble, and not to one particular configuration. Since each step (from any configuration), which passes through $\vec{r}$ changes the height of the ensemble envelope by a/N, the continuous height profile obeys the evolution equation

$$\frac{\partial h(\vec{r},t)}{\partial t}=-\nabla h_{-\hat{v}}(\vec{r},t)\cdot\vec{v}\left(C_{\vec{r},t}\right). \tag{2.4}$$

The above derivation of the evolution in the continuum is not valid at local extrema of the surface, because generally one cannot define a unique equal-height contour line which passes through such a point. To avoid the problem, we define $\partial h/\partial t$ at local extrema as the limit of the height time derivative as one approaches these points. This limiting procedure is justified, since there are no microscopic realizations of the surface with steps exactly at the local extrema.

At this point we emphasize that the Configurational Continuum evolution is formally identical to the evolution of the discrete step model. This statement is almost trivial, since the definition of Eq. (2.4) follows the envelope of the ensemble of configurations, and each configuration evolves with step velocities calculated from the discrete step model. Thus Eq. (2.4) is exact. Moreover, the use of directional derivatives in the derivation of Eq. (2.4) makes it valid even at singular surface regions such as corners or facet edges. Similarly to other continuum models it is solved numerically by discretization of space, which is the only approximation involved in such solutions.

What is the relation between Configurational Continuum and conventional continuum models? In regions where $h(\vec{r},t)$ is analytic, the evolution equation (2.4) reduces to the continuity equation

$$\frac{\partial h(\vec{r},t)}{\partial t} = -\nabla h(\vec{r},t)\cdot\vec{v}\left(C_{\vec{r},t}\right) \ . \tag{2.5}$$

If $h(\vec{r},t)$ is sufficiently smooth, $\vec{v}\left(C_{\vec{r},t}\right)$ can be approximated as a local function of h and its spatial derivatives, as is commonly done in conventional continuum models. Making this approximation will therefore recover the conventional continuum approach. We can conclude that in analytic surface regions the conventional continuum approach approximates the Configurational Continuum model and that the approximation quality depends on the smoothness of the surface. However, near corners, facets or regions where the profile is not smooth, one cannot reconstruct the microscopic step configuration from the local value of h and its spatial derivatives. In these regions $\vec{v}\left(C_{\vec{r},t}\right)$ contains non local information and as a result Eq. (2.4) cannot even be written as a differential equation.

Is there any computational gain in using such a continuum model? After all, we replaced a discrete model, which follows the evolution of a single microscopic step configuration, by a model which follows a whole ensemble of step configurations. The key point is that we do not have to follow all the steps of all configurations. To calculate $\partial h(\vec{r},t)/\partial t$, it is enough to locally follow the single configuration which has a step that passes trough $\vec{r}$ at time t. In addition, the continuum evolution equation is solved on a grid, and the density of grid points can be very small in regions where the continuous height profile is smooth. The smoothness of the profile allows very accurate interpolation between these points. Only near singular points or lines we have to use a rather dense grid, and there is no computational gain in these regions. In practice, the total number of grid points used can be orders of magnitude smaller than the number of points one has to use in order to follow the evolution of a single microscopic step configuration.

So far we ignored the possibility of island or void nucleation. It is possible to include island or void nucleation in our model provided that we have a microscopic description for these events which determines the nucleation probability in a given step configuration. Within our continuum approach, the nucleation probability at a point on the continuous surface is the ensemble average of the microscopic nucleation probabilities at this point. For demonstration proposes we consider a simple model where the probability for the nucleation of an island on a terrace grows as the square of the local concentration of diffusing adatoms. Information regarding the values of terrace adatom concentrations is already contained in the underlying step flow model Eq. (2.1), since it is used in the calculation of adatom fluxes into and out of steps.

3. Numerical solutions of the Configurational Continuum

We now apply our approach to a few simple cases. First, we consider a conic structure which consists of circular concentric steps. This crystalline cone was studied in Refs. [12, 13] where we wrote a one-dimensional step flow model for the step radii in the absence of growth flux. In the diffusion limited case where adatom diffusion across terraces is the rate limiting process, the equation of motion for the step radii r_n read:

$$\begin{aligned} \frac{dr_1}{dt} &= \frac{D_s C_\infty^{eq}\Omega}{k_B T r_1}\frac{\mu_1-\mu_2}{\ln\left(r_1/r_2\right)}\,, \\ \frac{dr_n}{dt} &= \frac{D_s C_\infty^{eq}\Omega}{k_B T r_n}\left(\frac{\mu_n-\mu_{n+1}}{\ln\left(r_n/r_{n+1}\right)}-\frac{\mu_{n-1}-\mu_n}{\ln\left(r_{n-1}/r_n\right)}\right)\,, \quad n>1\,, \end{aligned} \tag{3.1}$$

with the step chemical potentials μ_n given by

$$\mu_n = \frac{\Omega\Gamma}{r_n} + \Omega G\left[\frac{2r_{n+1}}{r_{n+1}+r_n}\cdot\frac{1}{\left(r_{n+1}-r_n\right)^3}-\frac{2r_{n-1}}{r_n+r_{n-1}}\cdot\frac{1}{\left(r_n-r_{n-1}\right)^3}\right]\,. \tag{3.2}$$

In the above expressions D_s is the adatom diffusion constant, Ω is the atomic area of the crystal and C_∞^{eq} is the equilibrium concentration in the vicinity of a straight isolated step. Γ is the step line tension, G is the step-step interaction strength, T is the temperature and k_B is the Boltzmann constant. Eq. (3.2) can be used for calculating the chemical potential of the top step, μ_1, by omitting the second interaction term.

Numerical integration of the above step model shows that the cone decays through the collapse of individual islands. During the decay a facet develops at the top of the cone with a radius that grows with time as $t^{1/4}$. Similar equations can be written in the presence of growth flux. With flux, the cone grows except at the peak which initially decays and then saturates. A facet forms at the peak after saturation.

The continuum model we solved in the context of this example is a fully two dimensional model, which can, in principle, develop non radially symmetric

morphologies. The microscopic dynamics we used were a two dimensional generalization of the microscopic equations for step radii of the discrete one dimensional model given above. In particular the step chemical potential was generalized to

$$\mu\left(\vec{r}\right)=\Omega\Gamma\kappa\left(\vec{r}\right)+\Omega G\left(\frac{\exp\left[\frac{|\vec{r}_d-\vec{r}|\cdot\kappa(\vec{r}_d)}{2}\right]}{\left|\vec{r}_d-\vec{r}\right|^3}-\frac{\exp\left[-\frac{|\vec{r}_u-\vec{r}|\cdot\kappa(\vec{r}_u)}{2}\right]}{\left|\vec{r}_u-\vec{r}\right|^3}\right)\ , \tag{3.3}$$

where $\kappa\left(\vec{r}\right)$ is the local step curvature. $\vec{r}_d$ and $\vec{r}_u$ are the coordinates at which the lower and upper neighboring steps are closest to the step at $\vec{r}$. It is assumed that these neighbors have the same sign as the step at $\vec{r}$ and that steps of opposite signs do not interact (in which case the relevant interaction terms in Eq. (3.3) are omitted). This expression was derived assuming an l^{-2} repulsion between two segments of two different steps which are separated by a distance l. Under this assumption, Eq. (3.3) is exact to first order in the curvature of neighboring steps and qualitatively captures the interaction when they have large curvatures.

The equations describing adatom diffusion on terraces were solved assuming the steps at $\vec{r}$, $\vec{r}_d$ and $\vec{r}_u$ are circular and concentric and that the radius of the step at $\vec{r}$ is $1/\kappa(\vec{r})$. Any microscopic dynamics, such as a full solution of the diffusion equation on each terrace, or a more detailed calculation of the interactions between steps can easily be used in the framework of our model. For the sake of demonstrating the validity of Configurational Continuum the simple dynamics we chose are sufficient.

Figure 2 shows a comparison between a numerical solution of the discrete step model and a cross section from the two dimensional solution of our continuum model in the absence of growth flux and when nucleation of new steps is not allowed. Clearly the continuum model captures the main features of the surface evolution. In particular the width and height of the top facet are in excellent agreement with the discrete model. Fig. 3 shows a similar comparison in the presence of growth flux. Again the agreement is quite impressive. In this case we allowed new islands to nucleate and our simulation indicates that nucleation events occur on the top facet once it becomes large enough. There is hardly any nucleation on the finite slope regions, because the steps there efficiently absorb the excess material. Figure 3(c) shows an island on the top facet, which nucleated and started growing.

We now turn to the more demanding example of bidirectional sinusoidal grating relaxation. Here the initial surface height profile of wave length L is given by

$$h_L(\vec{r},t=0)=h_0\sin\left(\frac{2\pi x}{L}\right)\sin\left(\frac{2\pi y}{L}\right)\ .$$

The relaxation of this profile towards a flat surface was studied by Rettori and Villain [20], who gave an approximate solution to a step flow model, in the limit where the interaction between steps can be neglected with respect to the step line tension. The decay of bidirectional sinusoidal profiles was also studied numerically

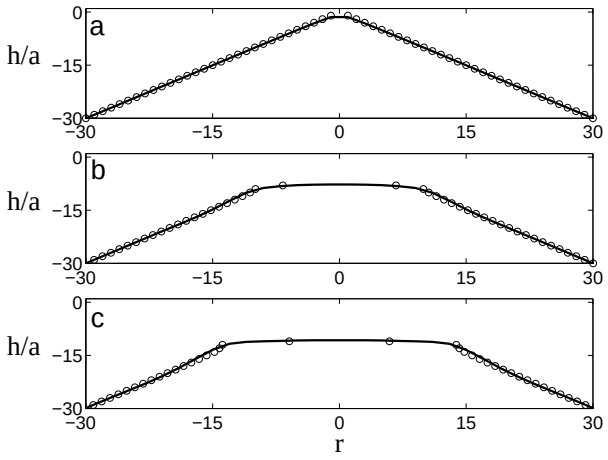

FIGURE 2. Decay of a crystalline cone. The solid line shows a cross section of the two dimensional solution of Eq. (2.4). Circles show the surface evolution according to the one dimensional step flow model Eq. (A.9). (a) is the initial morphology and (b) and (c) show the surface at later times.

[18]. We now apply our model to this problem assuming diffusion limited kinetics without deposition flux or island nucleation.

For weak interactions between steps, the surface height evolves according to $\partial h_L/\partial t \propto \nabla^2\kappa \sim L^{-3}$, where κ is the step curvature. We therefore expect the following scaling law for $h_L(\vec{r},t)$:

$$h_L(\vec{r},t) = h_{L=1}(\vec{r}/L, t/L^3)\ . \tag{3.4}$$

Figure 4 shows the data collapse of cross sections of profiles resulting from our continuum model. The different symbols correspond to profiles of different wave lengths at time $t = t_0 L^3$ for some fixed t_0. The quality of the data collapse shows that the scaling scenario (3.4) holds very accurately. Note that large facets have developed at the surface extrema, and they are connected by very steep slopes. This shape does not agree with Rettori and Villain's heuristic argument [20], which predicts that facets appear also near $h = 0$ lines. Nevertheless, their prediction that after a short transient the amplitude of the height profile decays as t/L^3 is in agreement with both Eq. (3.4) and our numerical solutions.

Figure 5 shows results for a much stronger repulsive interactions between steps, where the scaling law (3.4) clearly does not hold. Fig. 5 (a) shows profiles of different wavelengths which have relaxed to half of the initial amplitude. Here profiles with a smaller wavelength have small facets and moderate slopes. This happens because repulsion between steps becomes increasingly important as the profile wavelength is reduced. At long wavelengths the weak step-step interaction

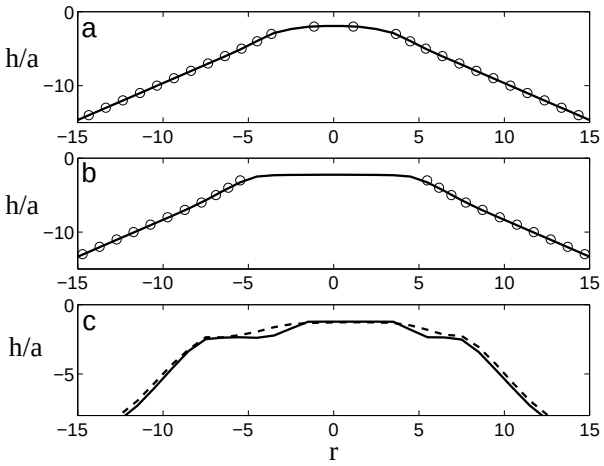

FIGURE 3. Evolution of a crystalline cone under growth conditions. The lines show cross sections of the two dimensional solution of Eq. (2.4). Circles show the surface evolution according to the one dimensional step flow model. The initial shape is the exact cone shown in Fig. 2 (a). (a) and (b) show the generation and evolution of a facet at the top at later times. (c) shows an island which nucleated (solid) and grew (dashed) on the top facet. Here no comparison is made with the step flow model.

limit of Fig. 4 is recovered. Fig. 5 (b) shows the different amplitudes as a function of scaled time t/L^3.

4. Conclusions

We proposed a novel continuum model for the evolution of sub roughening crystal surfaces. Our model, which we term Configurational Continuum, is derived directly from the underlying dynamics of atomic steps. Unlike conventional continuum models, Configurational Continuum is fully consistent with the step dynamics and is capable of handling singular surface features such as facets and corners.

The key idea in our model is to view the continuous surface profile as the envelope of an ensemble of step configurations which are all consistent with the continuous profile. Knowing the ensemble envelope, it is always possible to reconstruct individual configurations and evolve them in time. This evolution of individual configurations determines the evolution of the ensemble envelope which within our model is interpreted as the evolution of the profile. The continuum limit in our model is naturally realized because the continuous profile induces a continuum of possible step configurations.

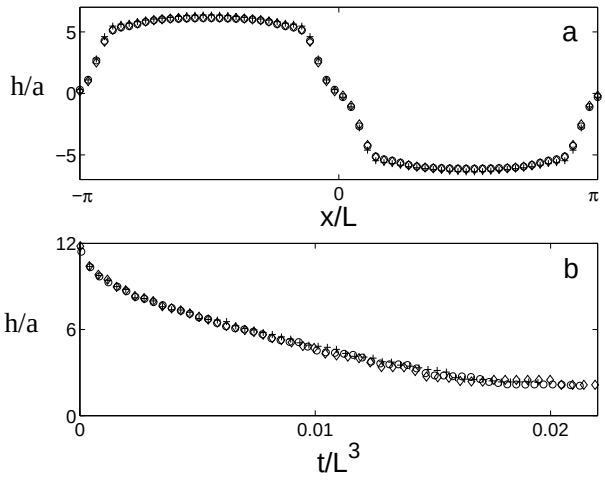

FIGURE 4. Data collapse in the evolution of bidirectional sinusoidal profiles with different wave lengths when the repulsive interaction between steps is very weak. Wave lengths shown are $L = 64$ (circles), $L = 128$ (squares) and $L = 256$ (triangles). a) Cross sections of the profiles with different wave lengths measured at time $t = t_0 L^3$. The cross sections are along the $y = -L/4$ line (peak to valley). b) Amplitude decay of the different wave lengths as a function of scaled time t/L^3.

Like other continuum models, Configurational Continuum has a computational advantage over the underlying discrete step model. When solved on a computer, it is possible to use a sparse grid in regions where the profile is very smooth. However, near corners or facets our model requires a fine discretization grid. The fine grid is necessary in order to faithfully reconstruct the step configurations which are possible near a singular point. Our model thus has the important property of being capable of describing step flow on different scales in a consistent way. In smooth surface regions, Configurational Continuum provides a coarse grained numerical description of surface dynamics. However it is still capable of accounting for the unique behavior of steps near singular points or lines.

The problem of connecting between different scales in dynamical systems is not limited to the evolution of surfaces. This problem is widespread in physics, engineering and biology as well as in other fields. Our hope is that the ideas at the basis of Configurational Continuum can be applied in other multi-scale problems.

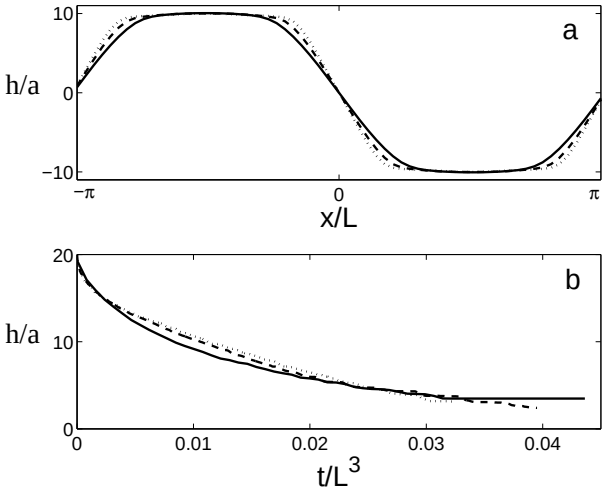

FIGURE 5. Bidirectional sinusoidal profiles in the case of stronger step-step interactions. Wave lengths shown are $L = 64$ (solid), $L = 128$ (dashed) and $L = 192$ (dotted). a) Cross sections of the profiles with different wave lengths which have relaxed to half of their initial amplitude. The cross sections are along the $y = -L/4$ line (peak to valley). b) Amplitude decay of the different wave lengths as a function of scaled time t/L^3.

Appendix A. Failure of the cusp rounding method.

In this appendix we give an example which shows how rounding of the surface free energy cusp can lead to erroneous solutions for surface evolution. As an example system we again choose the crystalline cone studied in Refs. [12, 13]. For simplicity we consider the diffusion limited case. This system is convenient since it exhibits scaling. In the scaling limit conventional continuum modelling of the cone becomes exact [12, 13] and we can concentrate on effects introduces by the cusp rounding method. We start by solving a model with a rounded free energy cusp and later compare the solution of this model with the relevant discrete step model and with the solution of the Configurational Continuum.

In the conventional continuum approach, the continuous free energy density of sub roughening surfaces has a cusp singularity at the high symmetry orientation. In a coordinate system where (x, y) is the high symmetry plane and $h(x, y)$ is the surface profile, the projected (on (x, y)) surface free energy density assumes the form [21]:

$$\mathcal{F}(x,y) = \mathcal{F}_0 + \Gamma |\nabla h(x,y)| + \frac{G}{3} |\nabla h(x,y)|^3 \ . \tag{A.1}$$

This form is the continuum analog of the free energy of an array of steps with line tension Γ and an inverse square repulsive step-step interaction of strength G.

The singular nature of the surface free energy complicates the modelling of surface evolution. Several authors have tried to overcome this problem by rounding the cusp with a small parameter α:

$$\mathcal{F}_\alpha(x,y) = \mathcal{F}_0 + \Gamma\left[(\nabla h(x,y))^2 + \alpha^2\right]^{1/2} + \frac{G}{3}\left[(\nabla h(x,y))^2 + \alpha^2\right]^{3/2} . \quad \text{(A.2)}$$

The hope behind this regularization scheme is that in the limit $\alpha \to 0$ the resulting model captures the correct surface dynamics.

Surface dynamics is derived from $\mathcal{F}_\alpha$ as follows. Taking the functional derivative of $\mathcal{F}_\alpha$ we obtain the surface chemical potential:

$$\mu_\alpha = \frac{\delta \mathcal{F}_\alpha}{\delta h} = -\Omega\left(\frac{\partial}{\partial x}\frac{\partial \mathcal{F}_\alpha}{\partial h_x} + \frac{\partial}{\partial y}\frac{\partial \mathcal{F}_\alpha}{\partial h_y}\right) , \quad \text{(A.3)}$$

where $h_x = \partial h/\partial x$ and $h_y = \partial h/\partial y$. For a radially symmetric profile $h(r,t)$ we find that

$$\mu_\alpha = -\frac{\Omega}{\sqrt{h_r^2+\alpha^2}}\left[\left(\frac{h_r}{r} + h_{rr}\right)\left(\Gamma + G\left(h_r^2+\alpha^2\right)\right) + h_r^2 h_{rr}\left(G - \frac{\Gamma}{h_r^2+\alpha^2}\right)\right] , \quad \text{(A.4)}$$

where $h_r = \partial h/\partial r$ and $h_{rr} = \partial^2 h/\partial r^2$.

In diffusion limited kinetics variations in the chemical potential give rise to currents which are proportional to the chemical potential gradient. For our radially symmetric profile we can consider only the radial component of this current

$$J = -\frac{D_s \tilde{C}^{eq}}{k_B T}\frac{\partial \mu_\alpha}{\partial r} . \quad \text{(A.5)}$$

The dynamic equation for the profile can now be written using the continuity equation

$$\frac{\partial h}{\partial t} = -\Omega \cdot \nabla J = \frac{\Omega D_s \tilde{C}^{eq}}{k_B T}\frac{1}{r}\frac{\partial}{\partial r}\left(r\frac{\partial \mu_\alpha}{\partial r}\right) . \quad \text{(A.6)}$$

The $\alpha \to 0$ limit of Eq. (A.6) automatically gives the correct equilibrium crystal shapes because Eq. (A.2) goes to Eq. (A.1) in this limit. We want to check whether this limit also gives the correct (consistent with step flow) dynamics.

We applied Eq. (A.6) to a crystalline cone $h(r, t=0) \sim -r$. The similarity sign here indicates that the tip of the initial profile was smoothed in order to have an analytic surface. Analyticity at the origin was also used as a boundary condition for the surface evolution. Numerical solutions show that, at long times the profile slope obeys a scaling law

$$h_r(r,t) = -F(rt^{-1/4}) . \quad \text{(A.7)}$$

This behavior agrees with the scaling properties exhibited by a discrete step flow model of the same surface structure [12, 13]. In Fig. 6 we show the resulting scaled slopes (dots) for different values of the cusp rounding parameter α. These long time solutions are not sensitive to the initial smoothing of the cone. As α is reduced

we observe the appearance of a very flat region around the origin. This flat region supposedly becomes a true facet in the $\alpha = 0$ limit.

For small values of α, solutions of the dynamic equation (A.6) approach scaling very slowly. For this reason it becomes increasingly difficult to probe the $\alpha = 0$ scaling state. In order to reach smaller values of α we continued in the following way. We assumed that the scaling ansatz (A.7) holds and used it to transform Eq. (A.6) into an ordinary differential equation for the scaling function $F(\xi)$ in the scaling variable $\xi = rt^{-1/4}$. Replacing $h_r(r,t)$ in Eq. (A.6) by the scaling function $F(\xi)$ we obtain the following equation:

$$\begin{aligned} -\frac{1}{4}F' &= \frac{\Omega D_s \tilde{C}^{eq}}{k_B T}\frac{d}{d\xi}\left[\frac{1}{\xi}\frac{d}{d\xi}\left(\xi\frac{d\eta_\alpha}{d\xi}\right)\right] , \\ \eta_\alpha &= -\frac{\Omega}{\sqrt{F^2+\alpha^2}}\left[\left(\frac{F}{\xi}+F'\right)\left(\Gamma + G\left(F^2+\alpha^2\right)\right)\right. \\ &\qquad \left. + F^2F'\left(G - \frac{\Gamma}{F^2+\alpha^2}\right)\right] , \end{aligned} \tag{A.8}$$

with $F' = dF/d\xi$.

Solutions of the above equation for the large values of α agree with the scaling states of the dynamic equation (A.6). The dashed lines in Fig. 6 show the resulting scaling functions for smaller values of α. Finally in order to determine the $\alpha = 0$ limit we estimated the scaled position of the facet edge from the $\alpha \neq 0$ solutions. This position selects[12, 13] a unique scaling solution for the $\alpha = 0$ case of Eq. (A.8). The resulting scaling function is shown by the solid line in Fig. 6. By our procedure this function is an approximation for the true scaling function of the system according to the cusp rounding method.

The solid line in Fig. 6 should be compared with the behavior of a system of discrete steps. For this purpose we introduce the following step model:

$$\begin{aligned} \frac{dr_1}{dt} &= \frac{D_s C_\infty^{eq}\Omega}{k_B T r_1}\frac{\mu_1 - \mu_2}{\ln\left(r_1/r_2\right)} , \\ \frac{dr_n}{dt} &= \frac{D_s C_\infty^{eq}\Omega}{k_B T r_n}\left(\frac{\mu_n - \mu_{n+1}}{\ln\left(r_n/r_{n+1}\right)} - \frac{\mu_{n-1} - \mu_n}{\ln\left(r_{n-1}/r_n\right)}\right) , \quad n > 1, \\ \mu_n &= \frac{\Omega\Gamma}{r_n} + \Omega G\left[\frac{2r_{n+1}}{r_{n+1}+r_n}\cdot\frac{1}{\left(r_{n+1}-r_n\right)^3} + \frac{r_{n+1}}{\left(r_{n+1}^2 - r_n^2\right)^2}\right. \\ &\qquad \left. - \frac{2r_{n-1}}{r_n + r_{n-1}}\cdot\frac{1}{\left(r_n - r_{n-1}\right)^3} + \frac{r_{n-1}}{\left(r_n^2 - r_{n-1}^2\right)^2}\right] . \end{aligned} \tag{A.9}$$

This is the same step model studied in section 3 and in Refs. [12, 13] with modified step chemical potentials. The modification has a small effect on the model behavior and does not introduce any qualitative changes. In particular, this step model obeys the same scaling properties that were studied in Refs. [12, 13], i.e., the density of steps in this model scales according to $D(r,t) = F_{discrete}(rt^{-1/4})$. In addition,

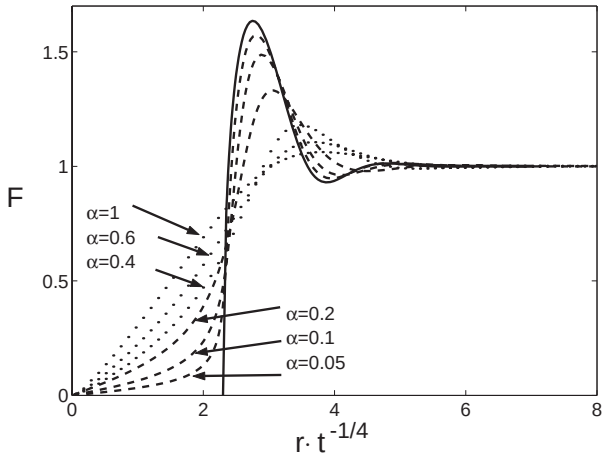

FIGURE 6. Scaling functions of the slope for different values of the cusp rounding parameter. Dots show scaling functions obtained from a direct solution of the dynamic equation (A.6). Dashed lines show solutions of the scaling equation (A.8). The solid line shows the estimated $\alpha = 0$ solution of Eq. (A.8).

applying the scaling analysis of Refs. [12, 13] to this modified step model results in an ordinary differential equation for the scaling function $F_{discrete}$ which is identical to the $\alpha = 0$ limit of Eq. (A.8). This fact gives us a basis for comparison between the step model and the cusp rounding scheme. Identifying the step density of the discrete model with the slope of the continuum model we can finally compare the limiting solution from the cusp rounding method with the scaled density of steps. In Fig. 7 we show that these two functions do not coincide. The scaled position of the facet edge in the cusp rounding method is about 40% larger than the one in the discrete system. This means that the difference between the two facets in real space diverges at long times. The height at the origin according to the cusp rounding method will suffer from the same errors. By assuming analyticity of the profile throughout the limiting procedure of the cusp rounding method, we have imposed erroneous boundary conditions at the facet edge.

Figure 7 also shows a one dimensional solution of the Configurational Continuum model for this cone system. The Configurational Continuum model predicts scaling of the slope as well. The discrepancy between the resulting scaling function and the discrete step system is much smaller and is consistent with what one would expect from discretization errors.

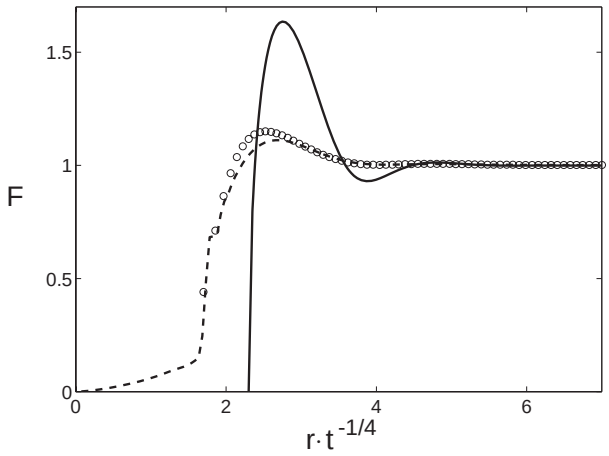

FIGURE 7. Comparison between the scaling function predicted by the cusp rounding procedure (solid), scaling function from a one dimensional solution of the Configurational Continuum (dashed) and the scaled density of steps in the discrete model (circles).

References

[1] W. K. Burton, N. Cabrera and F. C. Frank, Philos. Trans. R. Soc. London, Ser. A **243**, 299 (1951).

[2] For general reviews see H.-C. Jeong and E. D. Williams, Surf. Sci. Rep. **34**, 171 (1999); E. D. Williams, Surf. Sci. **299/300**, 502 (1994).

[3] E. S. Fu, M. D. Johnson, D. -J. Liu, J. D. Weeks, and E. D. Williams, Phys. Rev. Lett. **77**, 1091 (1996).

[4] S. Tanaka, N. C. Bartelt, C. C. Umbach, R. M. Tromp, and J. M. Blakely, Phys. Rev. Lett. **78**, 3342 (1997).

[5] W. W. Mullins, J. Appl. Phys. **28**, 333 (1957).

[6] M. Ozdemir and A. Zangwill, Phys. Rev. B **42**, 5013 (1990).

[7] P. Nozières, J. Phys. I France **48**, 1605 (1987).

[8] F. Lançon and J. Villain, Phys. Rev. Lett. **64**, 293 (1990).

[9] M. Uwaha, J. Phys. Soc. Jpn. **57**, 1681 (1988).

[10] A. Chame, S. Rousset, H. P. Bonzel, and J. Villain, Bul. Chem. Commun. **29**, 398 (1996/1997).

[11] J. Hager and H. Spohn, Surf. Sci. **324**, 365 (1995).

[12] N. Israeli and D. Kandel, Phys. Rev. Lett. **80** 3300 (1998).

[13] N. Israeli and D. Kandel, Phys. Rev. B **60** 5946 (1999).

[14] N. Israeli and D. Kandel, Phys. Rev. B **62** 13707 (2000).

[15] N. Israeli, H.-C. Jeong, D. Kandel and J. D. Weeks, Phys. Rev. B **61** 5698 (2000).

[16] H. P. Bonzel, E. Preuss and B Steffen, Appl. Phys. A **35**, 1 (1984).
[17] H. P. Bonzel and E. Preuss, Surf. Sci. **336**, 209 (1995).
[18] M. V. Ramana Murty, Phys. Rev. B **62**, 17004 (2000).
[19] N. Israeli and D. Kandel, Phys. Rev. Lett. **88**, 116103 (2002).
[20] A. Rettori and J. Villain, J. Phys. (Paris) **49**, 257 (1988).
[21] M. M. Gruber and W. W. Mallins, J. Phys. Chem. Solids **28**, 875 (1966).

Navot Israeli
Department of Physics of Complex Systems, Weizmann Institute of Science, Rehovot, 76100, Israel.
e-mail: navot.israeli@weizmann.ac.il

Daniel Kandel
Department of Physics of Complex Systems, Weizmann Institute of Science, Rehovot, 76100, Israel.
e-mail: daniel.kandel@weizmann.ac.il